

Forecasting landslides using mobility functions: a case study from Idukki district, India

Minu Treasa Abraham ^{1*}, Neelima Satyam ¹, Biswajeet Pradhan^{2,3,4}

¹ Discipline of Civil Engineering, Indian Institute of Technology Indore, Indore, Madhya Pradesh, India; 453552, ; phd1901204011@iiti.ac.in (M.T.A.), neelima.satyam@iiti.ac.in (N.S.)

² Centre for Advanced Modelling and Geospatial Information Systems (CAMGIS), Faculty of Engineering and Information Technology, University of Technology Sydney, Sydney, PO Box 123, Australia; Biswajeet.Pradhan@uts.edu.au (B.P.)

³ Center of Excellence for Climate Change Research, King Abdulaziz University, P. O. Box 80234, Jeddah 21589, Saudi Arabia

⁴ Earth Observation Center, Institute of Climate Change, Universiti Kebangsaan Malaysia, 43600 UKM, Bangi, Selangor, Malaysia

Abstract:

Catastrophic landslides and associated destructions are increasing every year, because of the change in climatic conditions and land use patterns. The ecologically sensitive zones of Western Ghats are highly susceptible to landslides and require scientific attention in developing an efficient early warning system. Definition of empirical rainfall thresholds on local, regional or global scales is the most commonly followed method of forecasting rainfall induced landslides. The limitations associated with such thresholds demands for better forecasting performance, incorporating the effect of physical processes in the initiation of landslides. This study is an attempt to forecast landslides in Idukki district, using mobility functions. The function separates the impossible and certain mobilisation parts and forecasts whether landslides can occur or not. Based on the critical value of mobility function, two different warning levels are proposed for four different reference areas in the district. The study shows that the model is 97 % efficient in smaller areas with uniform topographical and geological conditions, and the performance is reduced as the area becomes larger, with varying topographical and geological properties. The model proves to be an effective landslide forecasting tool that can be integrated with a rainfall forecasting system, to develop an early warning system for the region.

Keywords: rainfall thresholds; early warning; landslides; Idukki

1. Introduction

Landslides are loss of soil or rock mass, denoted by their movement downslope, directly influenced by gravity. It is a major geohazard, which affects the hilly regions all over the world, resulting in severe

32 destruction. Many landslides are part of natural geological evolution [1]. Due to the population rise,
33 more hilly areas are now being inhabited, increasing the risk associated with landslides. In India, most
34 of the landslides occurs during monsoon season, because of severe rainfall events. The rainwater
35 reduces the shear strength of soil, leading to shear failure [2]. Such events occur within a short span of
36 time and result in severe destructions such as loss of properties, lives and disruption of transportation
37 and infrastructure facilities. The socio-economic setbacks caused by landslides demand for a strong
38 scientific intervention to reduce the risk associated with landslides.

39 Providing early warning for landslides forecasting is an effective risk reduction approach [3,4]. An early
40 warning can provide enough time before the landslide event to take necessary decisions and actions.
41 The authorities and the public should be prepared and well aware of the action plans for the successful
42 implementation of an operational Landslide Early Warning System (LEWS) [5]. The early warning
43 should be issued based on the occurrence of the triggering factor (rainfall) and the in-situ site conditions.
44 The possible slope failure should be foreseen, based on the historical data and physical conditions [6].

45 Understanding the soil properties and evaluating the stability of slopes is a critical geotechnical
46 problem, and requires sophisticated inputs regarding the physical, hydrological and shear strength
47 properties of soil [7]. Collecting such time dependent information with precision is a challenging task.
48 Such inputs are used in process-based models [8], where infiltration models are used to understand the
49 phreatic lines and the stability of slopes are calculated using infinite slope model [8,9]. Such analysis
50 can be conducted for site-specific studies where precise data can be collected through regular
51 monitoring [7]. When the study area is large, the spatial and topographical variability limits the
52 availability of reliable input data. Hence the most commonly followed method in forecasting landslides
53 is the definition of empirical rainfall thresholds [10].

54 Empirical thresholds are conventionally defined as a linear relationship between the rainfall parameters
55 on a two-dimensional plane [11–14]. The threshold line defines a critical condition beyond which
56 landslides are expected to happen in a region. The definition of thresholds is subject to the type of
57 landslides and the size of the study area. The information regarding the antecedent rainfall within an
58 interval of a few hours or days is crucial for the initiation of shallow landslides and for deep-seated
59 failures, the duration of antecedent rainfall to be considered can be much longer, up to a few months.
60 Considering the size, the thresholds can be defined for single hill slopes to a global scale. The variations
61 in geology, hydrology, morphology, and climatic conditions can affect the definition of thresholds as
62 the amount of rainfall required to trigger landslides is highly dependent on these factors. Empirical
63 models are simple and can be derived for any region using the historical data [11]. But they are often
64 associated with the limitations due to the simplifying assumptions [15]. Conceptual improvements and
65 timely updates are required for the possible use of empirical thresholds in LEWS [6,16,17].

66 In this study, mobility functions are used to define a threshold condition which can be considered as a
67 conceptual improvement to the conventional intensity-duration (ID) thresholds [15]. Such functions are
68 used in the development of Forecasting of Landslides Induced by Rainfall (FLaIR) model and have
69 been proven effective in forecasting landslides [18–21].

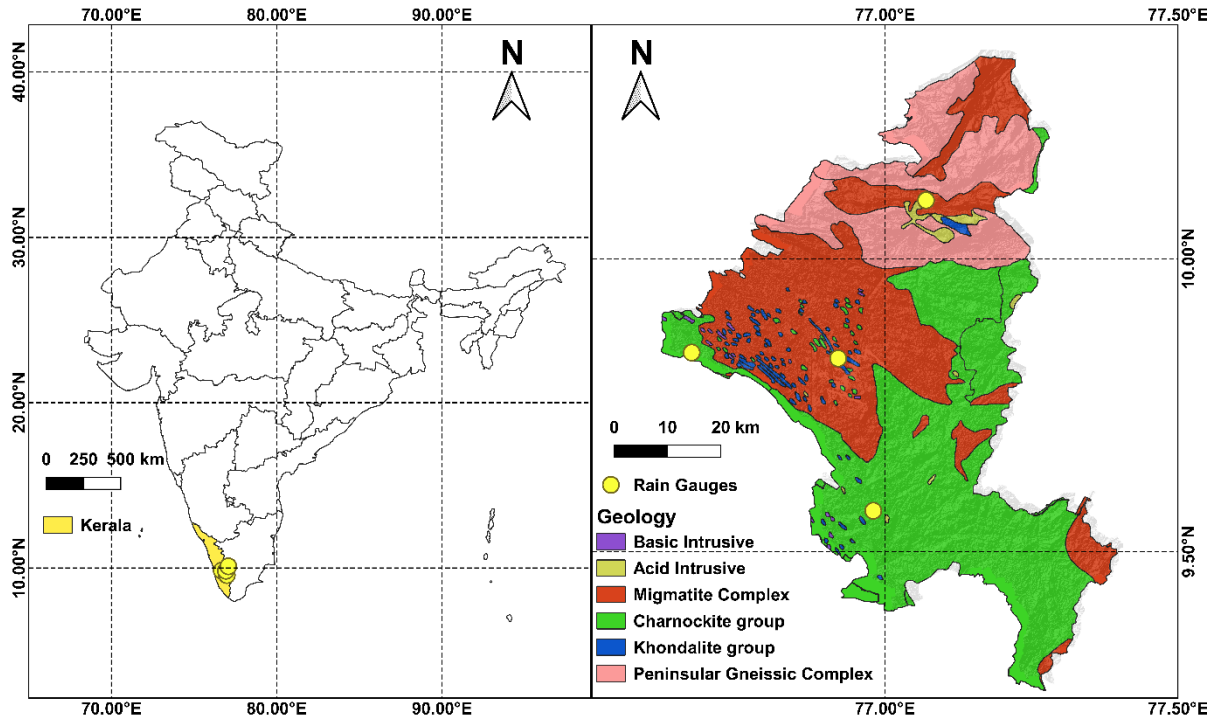
70 In India, the Himalayan belt [4,22–24] and the Western Ghats [25,26] are highly prone to landslides.
71 The Western Ghats is located along the Western coast of Indian Peninsular region and is the most
72 prominent orographic feature of the region. 47 % area of the state of Kerala in India is occupied by
73 Western Ghats [27]. The Western Ghats scarps are most susceptible to landslides as compared to the
74 other physiographic units [27]. The retreat of scarps along the weaker planes has formed the current
75 landscape of Western Ghats. Idukki is a hilly district in the Western Ghats and is highly prone to
76 landslides. A very recent landslide event in 2020 has resulted in the death of more than 60 people [28]
77 in the district and it is high time that an operational LEWS should be developed for this economically
78 backward district. This study is an attempt to make use of mobility functions for developing rainfall
79 thresholds for Idukki district.

80 **2. Details of the study area**

81 Idukki district is in the state of Kerala, whose district boundaries coincide with the limits of Western
82 Ghats. A major share of the district is covered by rugged mountains and forests. Low-lying regions are
83 not present in this hilly district whose elevation ranges from midlands to highlands. The highlands are
84 characterised by deep valleys and steep hills. The midland area comprises small hillocks, forming an
85 undulating topography. The hill ranges can be divided into the high ranges, plateau region and the
86 foothills. The midlands grade into the plateau in the narrow foothill zone, with an elevation ranging
87 from 80 m to 500 m. Foothills are narrow strips with width ranging from 2 km to 8 km. The most
88 significant physiographic unit of the district is the plateau region, with an elevation up to 1500 m.

89 The rocks of Peninsular Gneissic Complex (PGC), charnockite group and the migmatite group
90 constitute a major share of the geology of the region (Figure 1). Regionally folded and well foliated
91 granite gneiss represents the PGC in the northern part of the district. The widespread charnockite group
92 in the southern part is mostly massive, with banded varieties with compositions varying from
93 intermediate to felsic (Figure1). The migmatite complex in the central part is represented by hornblende
94 biotite gneiss and biotite gneiss.

95



96

97 Figure 1. Location details of the study area (a) India, (b) Geology map of Idukki (modified after [29])
 98 and location of rain gauges

99 The major income source of the district is agriculture and depends highly on the south-west and north-
 100 east monsoon for meeting the water requirements for agriculture. Most crops are rain-fed, but the
 101 monsoon season also triggers multiple landslides within the district, which results in destruction of lives
 102 and properties, including agricultural land. The eastern part of the region belongs to the rain shadow
 103 region of Western Ghats and the highest rainfall is recorded in the southern most rain gauge, located at
 104 Peerumed.

105 Most part of the district is drained by Periyar river, one among the major rivers in the state of Kerala.
 106 The river originates at the southeastern border of Idukki and flows west. The Idukki dam, one of the
 107 highest arch dams in Asia, is located across Periyar river. The district houses many reservoirs and
 108 contribute to the power supply and irrigation requirements of the state.

109 More than 60% of the surface soil is formed by organically rich forest loam soil. Such soil is formed by
 110 the weathering of rock under forest cover. The particles are fine grained and are suitable for plant
 111 growth, due to their high organic content. Lateritic soil is found in the midlands, which are well drained
 112 and have less organic content. The valleys of undulating terrain have a surface layer of hydromorphic
 113 soils, formed by the transportation and sedimentation of mass from nearby hill slopes. The particle sizes
 114 range from clayey to sandy. Alluvial soils are found along the riverbanks, as narrow strips. The topsoil,

115 in general, consists of clayey particles and have low permeability values. This increases the moisture
 116 holding capacity of the soil, making it suitable for agriculture. The highlands have recorded deep seated
 117 landslides while the midlands and plateau regions are suffering from cut slope failures and shallow
 118 landslides, majorly due to the recent land use changes that had happened in the region.

119 3. Methodology

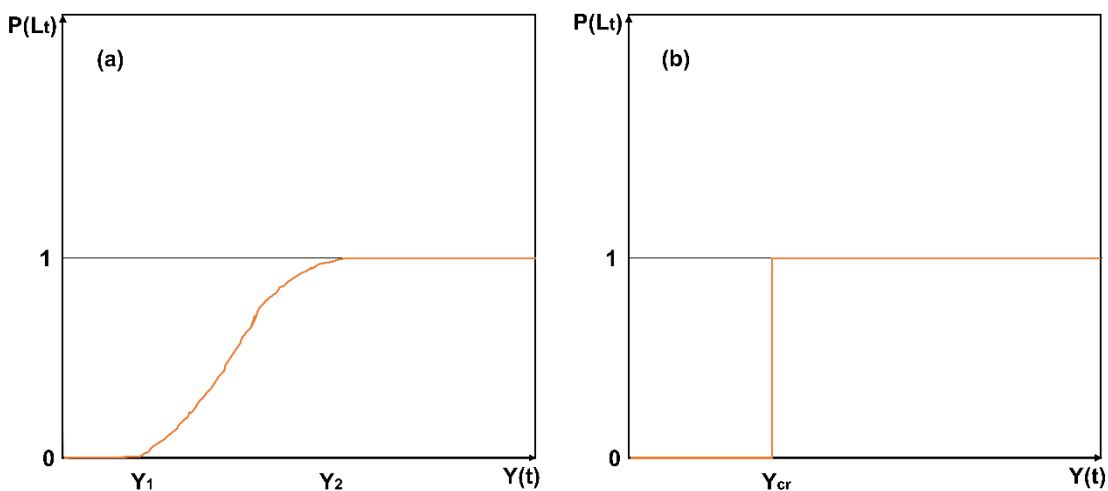
120 3.1 Mobility functions

121 Mobility functions ($Y(t)$) are generic functions, that can relate to the empirical rainfall thresholds, for
 122 forecasting the landslides [15]. The mobility functions depend upon the antecedent rainfall
 123 measurements and the definition depends upon historical data. It is assumed that the probability of
 124 occurrence of landslides at time t ($P(L_t)$) depends only on the mobility function $Y(t)$ and no
 125 modification has been occurred in the hillslope due to human or other factors [30]. Then the probability
 126 can be calculated as:

$$P(L_t) = \begin{cases} 0 & \text{if } Y(t) < Y_1 \\ g[Y(t)] & \text{if } Y_1 < Y(t) < Y_2 \\ 1 & \text{if } Y(t) > Y_2 \end{cases} \quad (1)$$

127

128 Where $g[]$ is a generic non-decreasing function which can take values from 0 to 1 as $Y(t)$ varies from
 129 Y_1 to Y_2 . The mobilisation is possible for values greater than Y_1 and it is certain when $Y(t) > Y_2$. The
 130 equation can be further simplified by using a certain value of $Y(t)$ as Y_{cr} where $Y_1 = Y_{cr} = Y_2$. This
 131 approximation simplifies the equation by adopting a critical value as threshold, separating impossible
 132 and certain mobilisation conditions.



133

134 Figure 2. Probability of occurrence of landslides vs mobility function (a) relationship based on Eq.

135 (1), (b) relationship with threshold condition Y_{cr}

136

137 For the definition of threshold condition, different criteria can be adopted, depending upon the severity
138 of landslide events. The most common criteria is the occurrence of one or more landslides [31,32]. In
139 the hydrological model FLaIR [15], mobility functions are estimated as a convolution between the
140 infiltration rate $I(\cdot)$ and a filter function $\psi(\cdot)$. The rate of infiltration is assumed to have a direct
141 relationship with the intensity of rainfall $I_r(\cdot)$ and it depends upon the type of soil. Since the
142 hydrological response is highly site specific, the model is best suited for local scale LEWS, however,
143 it can be successfully extended to regional scales [30] assuming the hydro-geological properties are
144 uniform. In this study, a simple relationship between $I(\tau)$ and $I_r(\tau)$ is used [15] as follows:

$$I(\tau) = \begin{cases} I_r(\tau) & \text{when } I_r(\tau) \leq I_{r0} \\ I_{r0} & \text{when } I_r(\tau) > I_{r0} \end{cases} \quad (2)$$

145 Where τ is the instantaneous time, varying from 0 to t . For simplification, we assume $I_{r0} = +\infty$ and
146 hence the mobility function can be directly related to the intensity of rainfall as :

$$Y(t) = \int_0^t \psi(t - \tau) I_r(\tau) d\tau \quad (3)$$

147 This formulation assumes a linear behaviour of the model. The choice of filter function is crucial in the
148 definition of mobility function. In this study, a gamma filter function is used to define the mobility
149 function. The filter function is given by the equation:

$$\psi(t) = \frac{\beta^\alpha}{\Gamma(\alpha)} t^{\alpha-1} e^{-\beta t} \quad t \geq 0, \alpha > 0, \beta > 0 \quad (4)$$

150 Where α is the shape parameter β (scale parameter) describes the hydrological response delay of the
151 occurrence of landslides with respect to the rainfall and defines the temporal scale, and $\Gamma(\cdot)$ is the
152 gamma function. The choice of transfer function depends upon the historical rainfall and landslide data.
153 For forecasting the occurrence of landslides, Eq. 4 can be divided into two parts given by:

$$Y(t) = \int_0^\tau \psi(t - \tau) I_r(\tau) d\tau + \int_\tau^t \psi(t - \tau) I_{r,pred}(\tau) d\tau \quad (5)$$

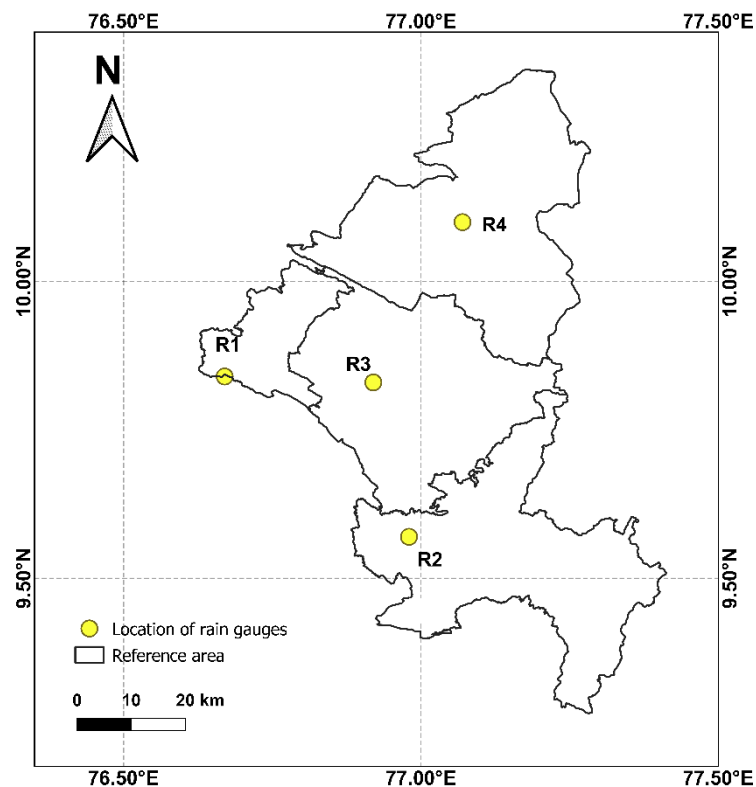
154 where $I_{r,pred}(\tau)$ is the forecasted rainfall. Thus, the mobility value at a future time t can be computed
155 using the second part of Eq. (6). This value can be compared with the critical value, to understand the
156 probability of occurrence of landslides.

157 The transfer function has been selected in such a way that the maximum value of mobility is obtained
158 on the day of slope failure. This study uses the rainfall and landslide data for Idukki district from 2010
159 to 2018. The rainfall data has been collected from India Meteorological Department [33] and the
160 landslide data has been collected from multiple sources including government agencies and media [32].
161 The data from 2010 to 2017 has been used for selecting the transfer function and the data of 2018 has

162 been used for the validation process, to verify the reliability of the model. Considering the whole year
163 will overestimate the performance of the model, due to high number of days without rainfall. Hence the
164 critical time duration, from June to November is considered for the validation of the model.

165 3.2 Developing Early Warning

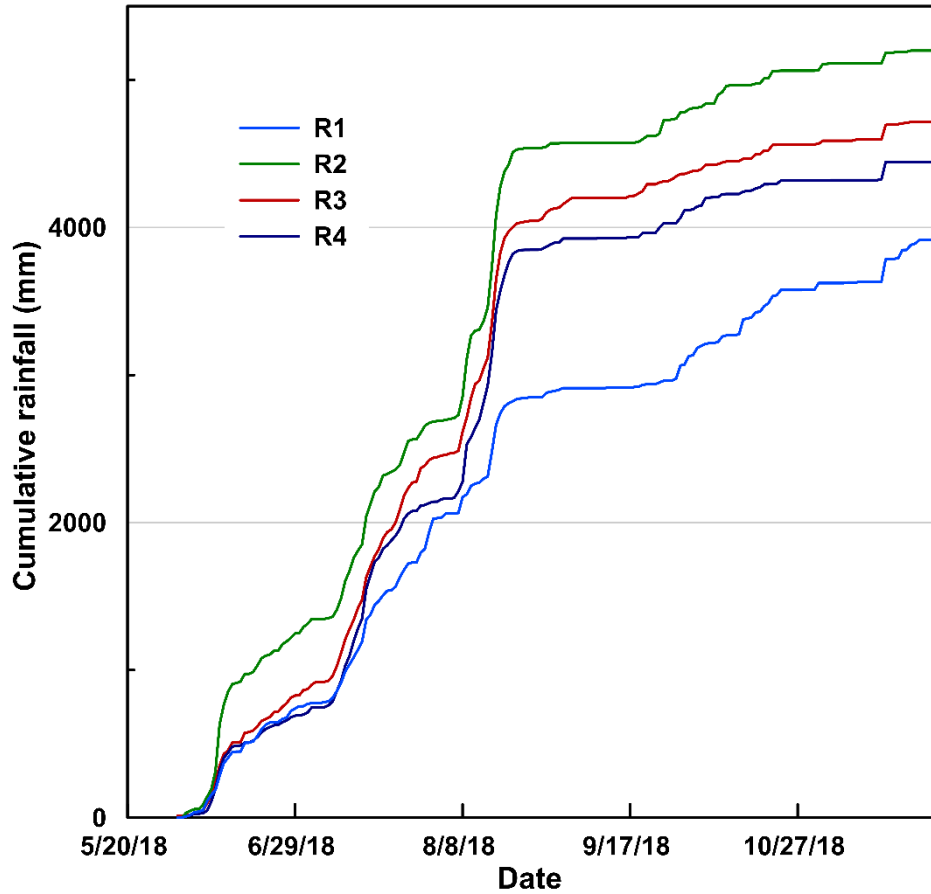
166 Depending upon the location of rain gauges, the district is divided into for different subzones, called
167 reference areas, and the rainfall is assumed to be uniform within the subzones. The division was done
168 using a proximity analysis by using the Thiessen polygon concept [32,34,35] and was improved further
169 using the administrative boundaries of the district (Figure 3). This division was done due to the variation
170 in meteorological conditions throughout the district. Also, the variations in topography is minimum
171 within each reference area, the area R1 represents the midland region of low elevation, R2 and R3 are
172 parts of hilly region in the eastern and central parts and R4 consists of highly rugged hills and valleys
173 of higher elevation. The rainfall received in the four reference areas is also varying (Figure 4). The
174 cumulative rainfall received during the validation period, from June to November 2018 is shown in
175 Figure 4. It can be observed that the maximum rainfall is recorded in R2, while R1 has recorded the
176 minimum rainfall.



177

178 Figure 3. The location of rain gauges and reference areas considered for issuing early warning

179 The boundaries of reference area are defined in such a way that the rain gauge within the area is the
 180 closest one to each point inside and the boundary coincides with the administrative boundary of the
 181 local government. This helps in the easy and straightforward operation of the early warning system.



182
 183 Figure 4. Cumulative rainfall during June to November, 2018

184 For developing an early warning system, multiple coefficients of the critical value can be used, to
 185 provide different levels of warning to the public [25,36–39]. This can be helpful in developing
 186 awareness among the public regarding different alert levels and actions to be taken for each level of
 187 warning. For defining alert levels, a coefficient is introduced, which is the ratio of mobility function at
 188 time t to the critical mobility value Y_{cr} , and can be expressed as:

$$C = \frac{Y(t)}{Y_{cr}} \quad (6)$$

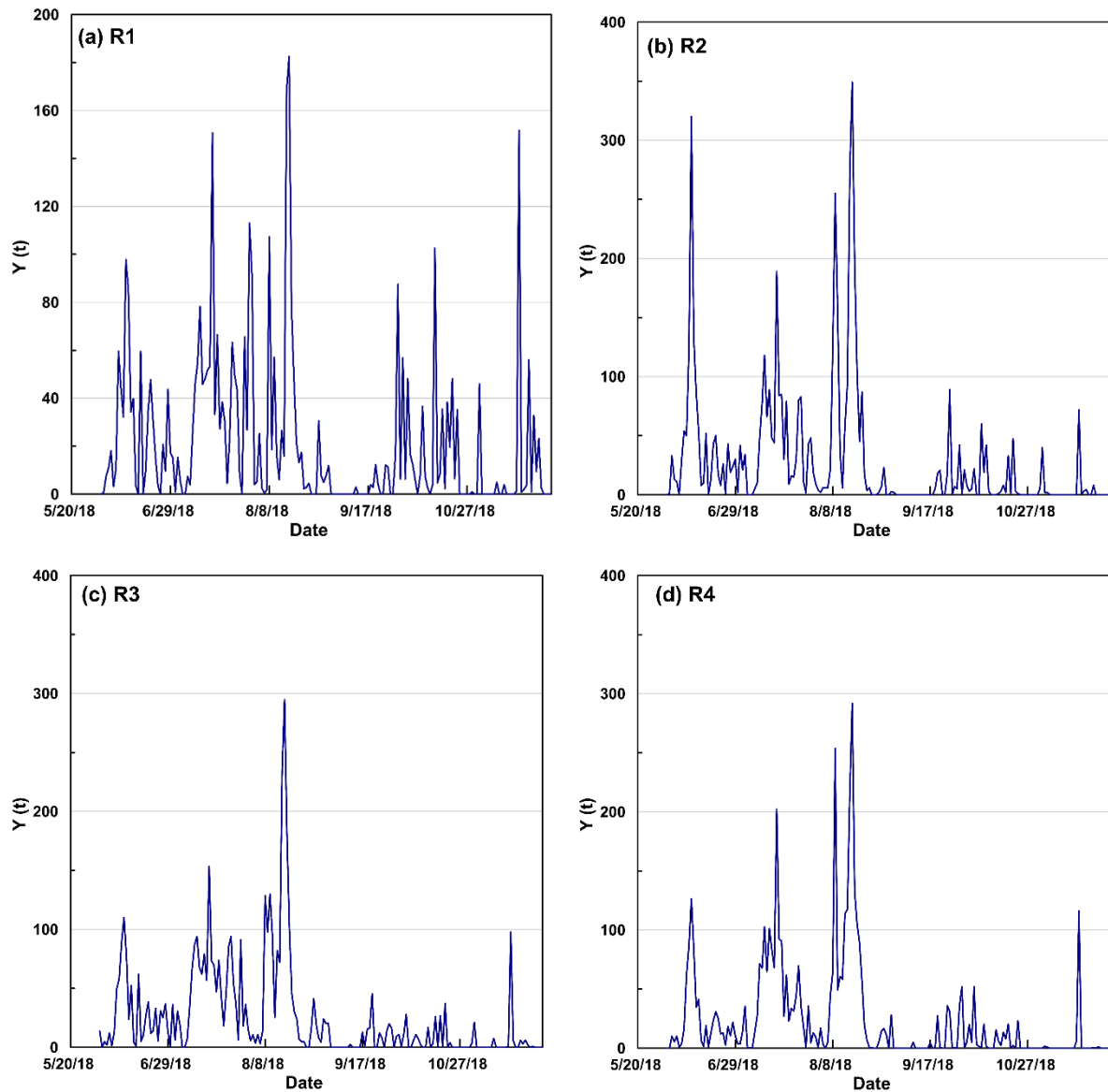
189
 190 The value of C has to be customised depending upon the history of rainfall and landslides in the region.
 191 The variation in climatic and lithological conditions of each reference area will lead to unique values
 192 of C for each reference area. In this study, two levels (C_1, C_2) of warning are defined for the study area,
 193 “Alert” and “Attention”. When “Attention” is issued on a day, landslide events of ordinary criticality

194 can be expected in the region and when “Alert” is issued, severe events can be expected. The forecasting
195 module must be integrated with a rainfall forecasting system for providing sufficient time of
196 intervention, so that necessary actions can be taken prior to the occurrence of landslides.

197 **4. Results**

198 The gamma function was used to define the mobility functions for forecasting landslides in Idukki,
199 India. The critical value of mobility function has been identified using the historical rainfall and
200 landslide data of the region, and customised warning levels were defined for each region. The mobility
201 functions for each reference area are shown in Figure 5. It can be observed that the maximum value of
202 mobility functions has been recorded in all areas during the time of 8th to 10th August 2018, when all
203 areas received a daily rainfall greater than 200 mm. The mobility functions are correlated with the daily
204 intensity of rainfall. The maximum value of mobility function has been recorded in R2, where the
205 district has received maximum rainfall.

206



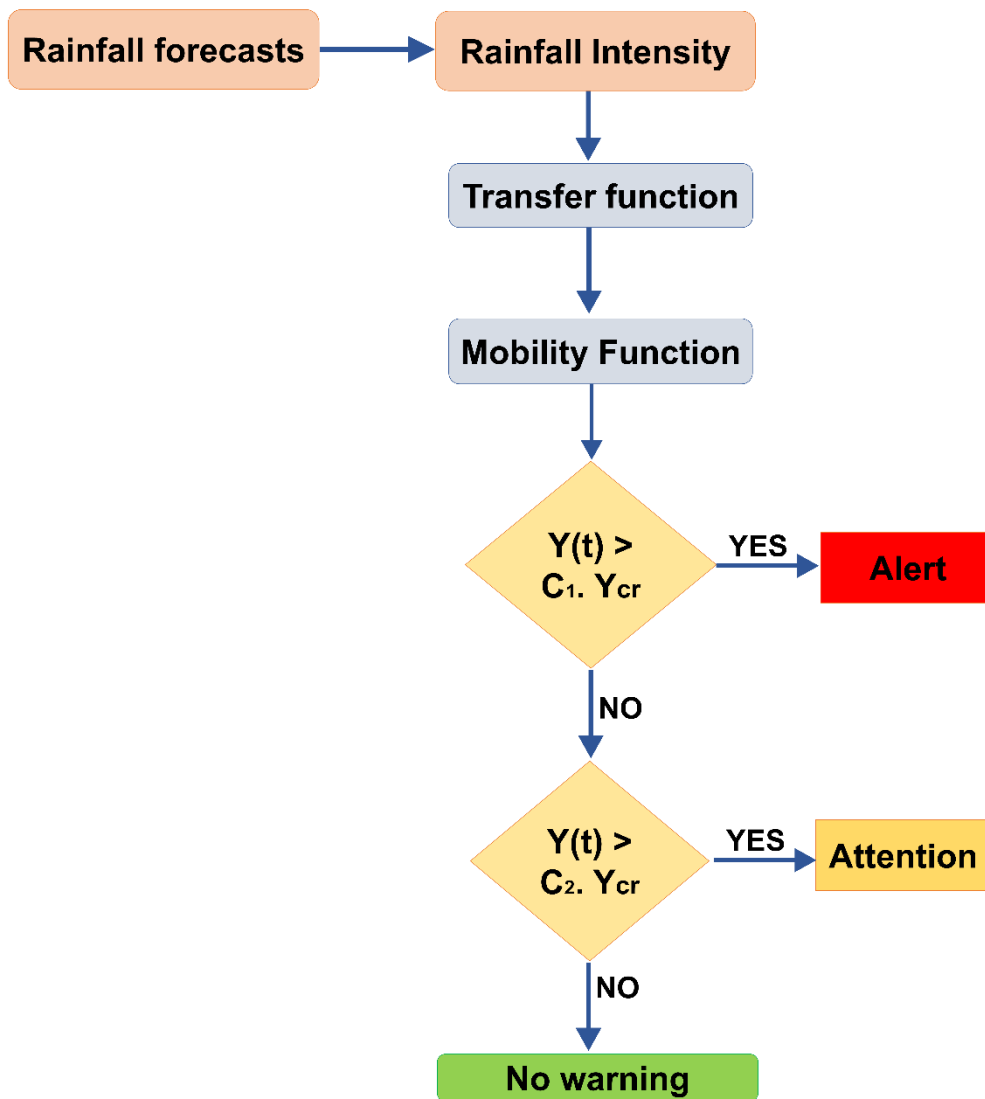
207

208 Figure 5. Mobility functions for different reference areas in Idukki district June to November 2018

209 The multipliers of critical mobility values for each area has been derived by using a trial-and-error
 210 procedure, so as to get a maximum number of true warnings and a minimum number of false warnings.
 211 Based on the procedure, an algorithm for issuing warning is proposed, as shown in Figure 6. First
 212 rainfall intensity in mm/day is calculated from rainfall forecasts and the value is used as an input for
 213 the transfer function. These values are compared with the critical mobility value for each area,
 214 multiplied with the coefficients (C_1, C_2) to issue warning. The algorithm first check if “Alert” has to be
 215 issued or are there chances for critical events. If the condition is not satisfied, it checks for the
 216 probability of occurrence of ordinary critical events (“Attention”). If both the conditions are not
 217 satisfied, no warning is issued for the day.

218

219



220

221 Figure 6. Algorithm proposed for the LEWS for issuing warnings based on mobility function

222

223 The performance of the algorithm shown in Figure 6 has been evaluated using a confusion matrix [40].
224 The warnings issued for 183 days from 1st June to 30th November 2018 has been compared with the
225 observed record of landslides in the study area, to count the number of statistical attributes like True
226 Positives (TP), False Positives (FP), False Negatives (FN) and True Negatives (TN). These values
227 indicate the performance of the model. When warning is issued and landslides have happened, it is
228 counted as TP and if no landslide has happened on a day with warning; it is counted as FP. Landslides
229 can happen on the days without warning also, and such days are counted as FN, while the days on which
230 no warning is issued and no landslide has happened are counted as TN. Both TP and TN are positive

231 outcomes, and FP and FN are negative outcomes. Our objective while customising the coefficients is
 232 to maximise the positive outcomes and minimise negative outcomes.

233 Table 1. Statistical attributes and customised coefficients for the reference areas

Reference area	TP	FP	FN	TN	Efficiency	Threshold	
						Alert	Attention
						C_1	C_2
R1	3	4	0	176	0.97	0.8	0.6
R2	4	4	0	175	0.97	0.8	0.4
R3	6	5	3	169	0.95	0.8	0.4
R4	8	4	6	165	0.95	0.8	0.4

234
 235 Efficiency is a term which is used to evaluate the performance of the model, which is expressed as the
 236 ratio of positive outcomes to the total number of outcomes. The more the efficiency, the better is the
 237 model. It can be understood from Table 1 that the efficiency of the model is greater than 95 % in all
 238 four reference areas. Also, the value of C_1 is obtained as 0.8 in all the cases. In the case of C_2 , the
 239 performance is better in R1 when the value is 0.6, but the optimum value is 0.4 in all other areas. For
 240 both the larger reference areas (R3 and R4), there are missed warnings, counted as FN, which reduces
 241 the performance of the model. Even though the efficiency is high for both R1 and R2, it should be
 242 observed that the ration of FP to TP is greater than or equal to 1 in both the cases. This means that out
 243 of the total warnings issued, at least 50 % are false alarms. This ratio is lesser in the case of areas R3
 244 and R4. Attempts have to be made to reduce this ratio, without increasing the number of FN, for the
 245 LEWS to be efficient.

246 5. Discussion

247 From the analysis, it was observed that the performance of the model, even with same coefficients
 248 (C_1, C_2) are different for different reference areas considered. The prediction performance of the model
 249 depends highly on the uniform meteo-hydrological properties of the region. This is because the
 250 hydrological response highly depends upon the properties of soil. When soil properties are varying, the
 251 relationship between precipitation and infiltration will also vary. It depends upon a number of factors
 252 ranging from slope of terrain to the properties of soil in the unsaturated conditions. But the methodology
 253 discussed in this study is only based on the historical data and does not consider the detailed site specific
 254 responses for each slope. The method is a conceptual improvement of the conventional empirical

255 thresholds, where the linear threshold is modified using a mobility function. No warnings are missed in
256 R1 and R2, where the topography and the geological conditions are relatively uniform. The efficiency
257 of the model is 97 % in both the regions. All the landslide events in these two regions were correctly
258 forecasted by the model, making it highly sensitive. Sensitivity of a model can be defined by the ratio
259 of TP to the sum of TP and FN. From Table 1, it can be understood that the model is 100 % sensitive
260 in R1 and R2 while the sensitivity is reduced in the case of R3 and R4.

261 For the days with no landslides, the results show that false warnings are issued by the model multiple
262 times during a monsoon. The term specificity deals with the prediction performance on non-landslide
263 days, and can be defined as the ratio of TN to the sum of TN and FP. In no reference area, the model
264 has given 100 % specific results. The forecast is always associated with false alarms. The rate of false
265 alarms is much lesser than the empirical thresholds, which makes the use of mobility functions a
266 possible tool for use in LEWS. The process of optimisation of coefficients for warning has reduced the
267 number of false alarms considerably. In regions R3 and R4, this came with the cost of many missed
268 alarms.

269 The use of mobility functions is a conceptual improvement from the conventional statistical thresholds
270 to a hydrological threshold, yet it is not associated with the complex process of evaluating physical
271 processes in detail. Though it overcomes the major limitation of the conventional empirical thresholds,
272 the high number of false alarms, the performance should be further improved for making the model
273 operational in R3 and R4. This can only be done with a higher rain gauge density and more precise
274 rainfall forecasts. The reference areas can be made smaller, so that the properties are uniform
275 throughout. Further research has to be done on this aspect, and the forecasting ability of the model can
276 be improved significantly. For large areas like Idukki district with sophisticated morphology, it is
277 difficult to do detailed physically based analysis and the empirical models are often associated with
278 very high false warnings. Hence the use of mobility functions is a promising approach in forecasting
279 the probability of occurrence of landslides within the study area.

280 The method can be exported to other parts of the world also, by using the historical landslide and rainfall
281 database for a particular study area. Thresholds can be developed on both local and regional scales. The
282 thresholds, when exported, should be customised for each study region based on its meteo-hydrological
283 properties and landslide histories. The threshold values and the relationship between precipitation and
284 infiltration will be different for each region, and the model has to be calibrated using regional specific
285 data.

286 **6. Conclusions**

287 A tool for forecasting the occurrence of landslides in the South Indian district of Idukki was derived by
288 using mobility functions. Unlike the conventional empirical thresholds, the mobility functions are
289 related to the rate of infiltration and calculates the probability of occurrence of a landslide event using

290 a mobility function. The model thus considers the complex hydrological processes using a generic
291 function and can be used for landslide forecasting, using the historical database.

292 The study shows that the use of mobility functions results only in a few false alarms for the study region.
293 The region was divided in to four reference areas, based on the location of rain gauges, and the
294 performance of the model was evaluated using the rainfall and landslide data from June to November
295 2018. The minimum efficiency obtained by the model is 95 % in regions R3 and R4, which have highly
296 varying topography and geology. The major limitations of the model are associated with the assumption
297 that the meteo-hydro-geological properties of the reference area remain the same. The model has very
298 good performance in regions R1 and R2, with an efficiency of 97 % and sensitivity 1.

299 The proposed model is a promising landslide forecasting tool that can be used in an operational LEWS,
300 along with a precise rainfall forecasting module. The study is significant for the region, which is highly
301 susceptible to landslides as the development of an efficient LEWS is a necessity for the safety of lives
302 and properties n hilly terrains.

303 **References**

- 304 1. DiBiagio, E.; Kjekstad, O. Early Warning, Instrumentation and Monitoring Landslides. In
305 Proceedings of the Asian Program for Regional Capacity Enhancement for Landslide Impact
306 Mitigation, RECLAIM II, 29th January - 3rd February 2007; Asian Disaster Preparedness
307 Center (ADPC) and Norwegian Geotechnical Institute (NGI): Phuket, Thailand, 2007.
- 308 2. Kuriakose, S.L. Physically-based dynamic modelling of the effect of land use changes on
309 shallow landslide initiation in the Western Ghats of Kerala, India, 2010.
- 310 3. Dikshit, A.; Satyam, D.N.; Towhata, I. Early warning system using tilt sensors in Chibo,
311 Kalimpong, Darjeeling Himalayas, India. *Nat. Hazards* **2018**, *94*, 727–741.
- 312 4. Dikshit, A.; Satyam, D.N. Estimation of rainfall thresholds for landslide occurrences in
313 Kalimpong, India. *Innov. Infrastruct. Solut.* **2018**, *3*.
- 314 5. Piciullo, L.; Calvello, M.; Cepeda, J.M. Territorial early warning systems for rainfall-induced
315 landslides. *Earth-Science Rev.* **2018**, *179*, 228–247.
- 316 6. Abraham, M.T.; Satyam, N.; Pradhan, B.; Alamri, A.M. Forecasting of landslides using rainfall
317 severity and soil wetness: A probabilistic approach for Darjeeling Himalayas. *Water*
318 *(Switzerland)* **2020**, *12*, 1–19.
- 319 7. Mirus, B.B.; Becker, R.E.; Baum, R.L.; Smith, J.B. Integrating real-time subsurface hydrologic
320 monitoring with empirical rainfall thresholds to improve landslide early warning. *Landslides*
321 **2018**, *15*, 1909–1919.

- 322 8. Baum, R.L.; Savage, W.Z.; Godt, J.W. *TRIGRS — A Fortran Program for Transient Rainfall*
323 *Infiltration and Grid-Based Regional Slope Stability Analysis*; 2008;
- 324 9. Iverson, R.M. Landslide triggering by rain infiltration. *Water Resour. Res.* **2000**, *36*, 1897–1910.
- 325 10. Segoni, S.; Piciullo, L.; Gariano, S.L. A review of the recent literature on rainfall thresholds for
326 landslide occurrence. *Landslides* **2018**, *15*, 1483–1501.
- 327 11. Guzzetti, F.; Peruccacci, S.; Rossi, M.; Stark, C.P. Rainfall thresholds for the initiation of
328 landslides in central and southern Europe. *Meteorol. Atmos. Phys.* **2007**, *98*, 239–267.
- 329 12. Melillo, M.; Brunetti, M.T.; Peruccacci, S.; Gariano, S.L.; Guzzetti, F. An Algorithm for the
330 objective reconstruction of rainfall events responsible for landslides. *Landslide Dyn. ISDR-ICL*
331 *Landslide Interact. Teach. Tools Vol. 1 Fundam. Mapp. Monit.* **2014**, *12*, 311–320.
- 332 13. Caine, N. The rainfall intensity-duration control of shallow landslides and debris flows: An
333 update. *Geogr. Ann. Ser. A, Phys. Geogr.* **1980**, *62*, 1–2, 23–27.
- 334 14. Aleotti, P. A warning system for rainfall-induced shallow failures. *Eng. Geol.* **2004**, *73*, 247–
335 265.
- 336 15. Capparelli, G.; Versace, P. FLAIIR and SUSHI: Two mathematical models for early warning of
337 landslides induced by rainfall. *Landslides* **2011**, *8*, 67–79.
- 338 16. Zhao, B.; Dai, Q.; Han, D.; Dai, H.; Mao, J.; Zhuo, L. Probabilistic thresholds for landslides
339 warning by integrating soil moisture conditions with rainfall thresholds. *J. Hydrol.* **2019**, *574*,
340 276–287.
- 341 17. Segoni, S.; Rosi, A.; Lagomarsino, D.; Fanti, R.; Casagli, N. Brief communication: Using
342 averaged soil moisture estimates to improve the performances of a regional-scale landslide early
343 warning system. *Nat. Hazards Earth Syst. Sci.* **2018**, *18*, 807–812.
- 344 18. Versace, P.; Capparelli, G.; De Luca, D.L. TXT-tool 2.039-4.1: FLAIIR Model (Forecasting of
345 Landslides Induced by Rainfalls). In *Landslide Dynamics: ISDR-ICL Landslide Interactive*
346 *Teaching Tools*; Springer International Publishing: Cham, 2018; pp. 381–389 ISBN
347 9783319577746.
- 348 19. Capparelli, G.; Tiranti, D. Application of the MoniFLAIIR early warning system for rainfall-
349 induced landslides in Piedmont region (Italy). *Landslides* **2010**, *7*, 401–410.
- 350 20. Capparelli, G.; Calabria, U.; Tiranti, D.; Calabria, U. Forecasting of landslides induced by
351 rainfall - F.La.I.R . hydrological model application on Piemonte Region (NW Italy). *Geophys.*
352 *Res. Abstr.* **2007**, *9*,02298.

- 353 21. Crosta, G.B.; Imposimato, S.; Roddeman, D.G. Numerical modelling of large landslides stability
354 and runout. *Nat. Hazards Earth Syst. Sci.* **2010**, *3*, 523–538.
- 355 22. Froude, M.J.; Petley, D.N. Global fatal landslide occurrence from 2004 to 2016. *Nat. Hazards*
356 *Earth Syst. Sci.* **2018**, *18*, 2161–2181.
- 357 23. Dikshit, A.; Satyam, N. Probabilistic rainfall thresholds in Chibo, India: estimation and
358 validation using monitoring system. *J. Mt. Sci.* **2019**, *16*, 870–883.
- 359 24. Dikshit, A.; Satyam, N.; Pradhan, B. Estimation of Rainfall - Induced Landslides Using the
360 TRIGRS Model. *Earth Syst. Environ.* **2019**.
- 361 25. Abraham, M.T.; Satyam, N.; Kushal, S.; Rosi, A.; Pradhan, B.; Segoni, S. Rainfall Threshold
362 Estimation and Landslide Forecasting for Kalimpong, India Using SIGMA Model. *Water* **2020**,
363 *12*, 1195.
- 364 26. Abraham, M.T.; Satyam, N.; Reddy, S.K.P.; Pradhan, B. Runout modeling and calibration of
365 friction parameters of Kurichermala debris flow, India. *Landslides* **2020**.
- 366 27. Kuriakose, S.L.; Sankar, G.; Muraleedharan, C. History of landslide susceptibility and a
367 chorology of landslide-prone areas in the Western Ghats of Kerala, India. *Environ. Geol.* **2009**,
368 *57*, 1553–1568.
- 369 28. Jose, J.P. Death by landslides in God's own country. *The Hindu* 2020.
- 370 29. Department of Mining and Geology Kerala *District Survey Report of Minor Minerals*;
371 Thiruvananthapuram, 2016;
- 372 30. Iiritano, G.; Versace, P.; Sirangelo, B. Real-time estimation of hazard for landslides triggered
373 by rainfall. *Environ. Geol.* **1998**, *35*, 175–183.
- 374 31. Berti, M.; Martina, M.L.V.; Franceschini, S.; Pignone, S.; Simoni, A.; Pizziolo, M. Probabilistic
375 rainfall thresholds for landslide occurrence using a Bayesian approach. *J. Geophys. Res. Earth*
376 *Surf.* **2012**, *117*, 1–20.
- 377 32. Abraham, M.T.; Pothuraju, D.; Satyam, N. Rainfall Thresholds for Prediction of Landslides in
378 Idukki, India: An Empirical Approach. *Water* **2019**, *11*, 2113.
- 379 33. India Meteorological Department India Meteorological Department (IMD) Data Supply Portal.
- 380 34. Abraham, M.T.; Satyam, N.; Rosi, A. Empirical Rainfall Thresholds for Occurrence of
381 Landslides in Wayanad, India. *EGU Gen. Assem.* **2020**, 5194.
- 382 35. Abraham, M.T.; Satyam, N.; Rosi, A.; Pradhan, B.; Segoni, S. The Selection of Rain Gauges
383 and Rainfall Parameters in Estimating Intensity-Duration Thresholds for Landslide Occurrence:

- 384 Case Study from Wayanad (India). *Water* **2020**, *12*, 1000.
- 385 36. Baum, R.; Godt, J.; Harp, E.; McKenna, J.; McMullen, S. Early warning of landslides for rail
386 traffic between Seattle and Everett, Washington, U.S.A. In Proceedings of the International of
387 Conference on Landslide Risk Management; Vancouver, 2005; pp. 731–740.
- 388 37. Rabuffetti, D.; Barbero, S. Operational hydro-meteorological warning and real-time flood
389 forecasting: The Piemonte Region case study. *Hydrol. Earth Syst. Sci.* **2005**, *9*, 457–466.
- 390 38. Martelloni, G.; Segoni, S.; Fanti, R.; Catani, F. Rainfall thresholds for the forecasting of
391 landslide occurrence at regional scale. *Landslides* **2012**, *9*, 485–495.
- 392 39. Segoni, S.; Rosi, A.; Fanti, R.; Gallucci, A.; Monni, A.; Casagli, N. A regional-scale landslide
393 warning system based on 20 years of operational experience. *Water (Switzerland)* **2018**, *10*, 1–
394 17.
- 395 40. Lagomarsino, D.; Segoni, S.; Rosi, A.; Rossi, G.; Battistini, A.; Catani, F.; Casagli, N.
396 Quantitative comparison between two different methodologies to define rainfall thresholds for
397 landslide forecasting. *Nat. Hazards Earth Syst. Sci.* **2015**, *15*, 2413–2423.
- 398
- 399